Available online at www.sciencedirect.com

SCIENCE DIRECT®

Journal of Controlled Release 104 (2005) 51–66

journal of controlled release

www.elsevier.com/locate/jconrel

Biodegradable polymer microneedles: Fabrication, mechanics and transdermal drug delivery

Jung-Hwan Park[a], Mark G. Allen[b], Mark R. Prausnitz[a,c,*]

[a]*The Wallace H. Coulter Department of Biomedical Engineering at Georgia Tech and Emory University, Georgia Institute of Technology, Atlanta, GA 30332, USA*

[b]*School of Electrical and Computer Engineering, Georgia Institute of Technology, Atlanta, GA 30332, USA*

[c]*School of Chemical and Biomolecular Engineering, Georgia Institute of Technology, Atlanta, GA 30332, USA*

Received 3 November 2004; accepted 2 February 2005
Available online 1 April 2005

Abstract

To overcome the skin's barrier properties that block transdermal delivery of most drugs, arrays of microscopic needles have been microfabricated primarily out of silicon or metal. This study addresses microneedles made of biocompatible and biodegradable polymers, which are expected to improve safety and manufacturability. To make biodegradable polymer microneedles with sharp tips, micro-electromechanical masking and etching were adapted to produce beveled- and chisel-tip microneedles and a new fabrication method was developed to produce tapered-cone microneedles using an in situ lens-based lithographic approach. To replicate microfabricated master structures, PDMS micromolds were generated and a novel vacuum-based method was developed to fill the molds with polylactic acid, polyglycolic acid, and their co-polymers. Mechanical testing of the resulting needles measured the force at which needles broke during axial loading and found that this failure force increased with Young's modulus of the material and needle base diameter and decreased with needle length. Failure forces were generally much larger than the forces needed to insert microneedles into skin, indicating that biodegradable polymers can have satisfactory mechanical properties for microneedles. Finally, arrays of polymer microneedles were shown to increase permeability of human cadaver skin to a low-molecular weight tracer, calcein, and a macromolecular protein, bovine serum albumin, by up to three orders of magnitude. Altogether, these results indicate that biodegradable polymer microneedles can be fabricated with an appropriate geometry and sufficient strength to insert into skin, and thereby dramatically increase transdermal transport of molecules.

Keywords: Microneedle; Transdermal drug delivery; Biodegradable polymer; Failure force

1. Introduction

Most drugs are administered in the form of pills or injections, but these methods of delivery are not

* Corresponding author. School of Chemical and Biomolecular Engineering, Georgia Institute of Technology, Atlanta, GA 30332, USA. Tel.: +1 404 894 5135; fax: +1 404 894 2291.
E-mail addresses: junghwan.park@gmail.com (J.-H. Park), mark.allen@ece.gatech.edu (M.G. Allen), mark.prausnitz@chbe.gatech.edu (M.R. Prausnitz).

0168-3659/$ - see front matter © 2005 Elsevier B.V. All rights reserved.
doi:10.1016/j.jconrel.2005.02.002

always optimal [1,2]. Medication taken orally must not only be absorbed successfully out of the intestine into the bloodstream, but also survive the harsh and enzyme-rich environments of the gastrointestinal tract and first pass through the liver. Drugs that cannot be taken as pills are usually administered by injection, which introduces the problems of pain, possible infection, and expertise required to carry out an injection. Both routes of delivery have added limitations as bolus delivery methods, where the full dose of drug is introduced into the body at once. To prevent the toxic and irritating effects of initial high doses and the sub-therapeutic effects as drug concentration decays at later times, pills and injections sometimes need to be administered multiple times per day or, in some cases, sustained-release formulations can be used.

As an alternative to pills and injections, transdermal drug delivery has been developed to slowly transport drugs into the body across the skin [3–5]. This approach avoids the limitations of oral and injection delivery mentioned above. Given these advantages, transdermal patches containing a dozen different drugs have been approved for use in the United States, including nicotine for smoking cessation and fentanyl for pain control [3]. These patches are typically made of polymer, contain a drug reservoir and adhesive layer, and provide steady, controlled drug delivery for up to a week. In addition, hundreds of topical formulations have been developed in the form of creams or ointments primarily for short-term, local treatment of the skin or neighboring tissues [4].

Despite these advantages, transdermal drug delivery is currently useful for only a small subset of drugs, because most compounds cannot cross the skin at therapeutic rates. The extraordinary barrier properties of the stratum corneum, the outer 10–15 μm of skin, generally permit transport only of small (<400 Da), oil-soluble molecules [6]. To address this limitation, a variety of methods to increase transdermal transport have been studied, including chemical enhancers, electric fields, ultrasound, and thermal methods [3,4,7]. Although still under active investigation, these enhancement methods have made only limited impact on medical practice to date.

A new approach to transdermal drug delivery that acts as a bridge between the user-friendliness of patches and the broad effectiveness of hypodermic needles has recently received attention [8–11]. By using needles of microns dimensions, termed microneedles, skin can be pierced to effectively deliver drugs, but do so in a minimally invasive and painless manner that lends itself to self-administration and slow delivery over time. Microneedles have been made primarily by adapting the technologies of the microelectronics industry to produce arrays of silicon, metal and, as described here, polymer needles. Solid microneedles have been shown to increase skin permeability by up to four orders of magnitude for compounds ranging in size from small molecules to proteins to nanoparticles [8,12]. In vivo studies have demonstrated delivery of oligonucleotides, desmopressin, and human growth hormone [13–15], reduction of blood glucose levels from insulin delivery [16], increase of skin transfection with DNA [17], and elicitation of immune response from delivery of DNA and protein antigens [18,19]. Hollow microneedles have also been shown to deliver insulin and reduce blood glucose levels [12,20,21].

Most microneedles previously presented have been made of silicon [22–24] or metal [15,25–27]. Although silicon is attractive as a common microelectronics industry substrate with extensive processing experience, it is relatively expensive, fragile, and unproven as a biocompatible material [28]. Many metals are cheaper, stronger and known to be biocompatible [29], which makes metal especially attractive for hollow needles that need structural strength [30]. Polymer microneedles have received limited attention [31], but also provide an inexpensive, biocompatible material that lends itself to mass production and may offer improved resistance to shear-induced breakage due to polymer viscoelasticity [32]. Previous microneedle fabrication methods have often been time consuming and expensive due to reliance on multi-step, cleanroom-intensive processes [33].

As a novel approach to microneedle fabrication, this study was motivated by the goal to make microneedles out of biodegradable polymers using mold-based fabrication methods that lend themselves to inexpensive and robust mass production. There do not appear to be previous publications describing the use of biodegradable polymers or micromolding to make polymer microneedles. Polylactic acid (PLA),

polyglycolic acid (PGA), and their co-polymers (PLGA) were selected as microneedle materials because these polymers have a long history of biocompatibility as resorbable sutures and are cost effective and mechanically strong [34]. To provide additional safety, biodegradable microneedles that might accidentally break off in the skin should safely degrade and eventually disappear. In this study, we present methods to fabricate microneedles using biodegradable polymers, measure needle mechanical properties, and assess their ability to increase transport across the skin.

2. Materials and methods

2.1. Microneedle fabrication processes

The process to fabricate biodegradable polymer microneedles is based on micromolding using high-aspect-ratio SU-8 epoxy photoresist or polyurethane master structures to form PDMS (polydimethyl siloxane) molds from which biodegradable polymer microneedle replicates are formed [12,35,36].

2.1.1. Beveled-tip master structures

Microneedles with beveled tips were fabricated by first creating a master structure from SU-8 epoxy using ultraviolet (UV) lithography (Fig. 1). SU-8 epoxy with photoinitiator (SU-8 100; MicroChem, Newton, MA) was coated to a thickness of 300–350 μm onto a silicon wafer (Nova Electronic Materials, Richardson, TX) and lithographically patterned into 100 μm diameter cylinders, which defined the shape of the desired needles. Although these cylinders were usually circular in cross-section, sometimes a different mask was used to create cylinders with a notch of 30-μm radius cut out of one side. These cylinders were arranged in an array, where the center-to-center spacing between cylinders in each row was 1400 μm and between each column was 400 μm. The array contained 20 cylinders in each row arranged in 6 columns for a total of 120 cylinders in an area of 9×9 mm.

The space between cylinders was filled with a sacrificial polymer (PLGA 85/15, Birmingham Polymers, Birmingham, AL) and the entire surface was coated with a 600-nm thick layer of copper by electron beam deposition (E-beam, CVC products, Rochester, NY). This copper layer was etched with acid ($H_2SO_4 : H_2O_2 : H_2O$ at a volumetric ratio of 1 : 1 : 10) to leave a pattern of rectangles with 0.6 mm width and 10 mm length that asymmetrically covered the tops of the epoxy cylinders and some of the sacrificial polymer on one side of each cylinder. Reactive ion etching (RIE; Plasma Therm, St. Peterburg, FL) partially removed the uncovered sacrificial layer and asymmetrically etched the tip of the adjacent epoxy cylinders. All remaining sacrificial polymer was removed by ethyl acetate (Aldrich, St. Louis, MO), leaving an array of epoxy cylinders with asymmetrically beveled tips.

2.1.2. Chisel-tip master structures

Chisel-tip microneedles were fabricated using a combination of wet silicon etching and reactive ion etching of polymers (Fig. 2). Silicon nitride was deposited onto a silicon wafer (<1,0,0>, Nova Electronic Materials) to a thickness of 4000 Å by chemical vapor deposition (PECVD, Plasma Therm) to make a hard mask to protect silicon against KOH etching. Next, the silicon nitride layer was lithographically patterned to expose a 15×15 array of square dots each measuring 100 μm in width with 600-μm center-to-center spacing. The exposed silicon nitride layer was removed using reactive ion etching and the photoresist was then removed using acetone. KOH (30 wt.%, Aldrich) heated to 80 °C was then applied to the wafer to etch inverted pyramid-shaped holes. Etching occurred along the crystal plane to form 55°-tapered walls terminating in a sharp point [37], which provide the chisel shape of the needle tips.

To form the shape of the needle shaft, SU-8 epoxy photoresist with photoinitiator was spin-coated onto the etched wafer to form a 500-μm thick film. A second mask was aligned with the wafer to expose the SU-8 coating to UV light in the same 15×15 array of square dots in vertical alignment with the silicon nitride pattern. After post-baking to crosslink the UV-exposed SU-8 on a hotplate (Brewer Science, Rolla, MO) for 30 min at 100 °C and then cooling, the non-crosslinked epoxy was developed with PGMEA to leave behind obelisk-shaped SU-8 structures with their tips still embedded in the silicon wafer.

To finally make master needle structures, the space between the obelisk structures was filled with PDMS (Sylgard 184, Dow Corning). The crosslinked SU-8

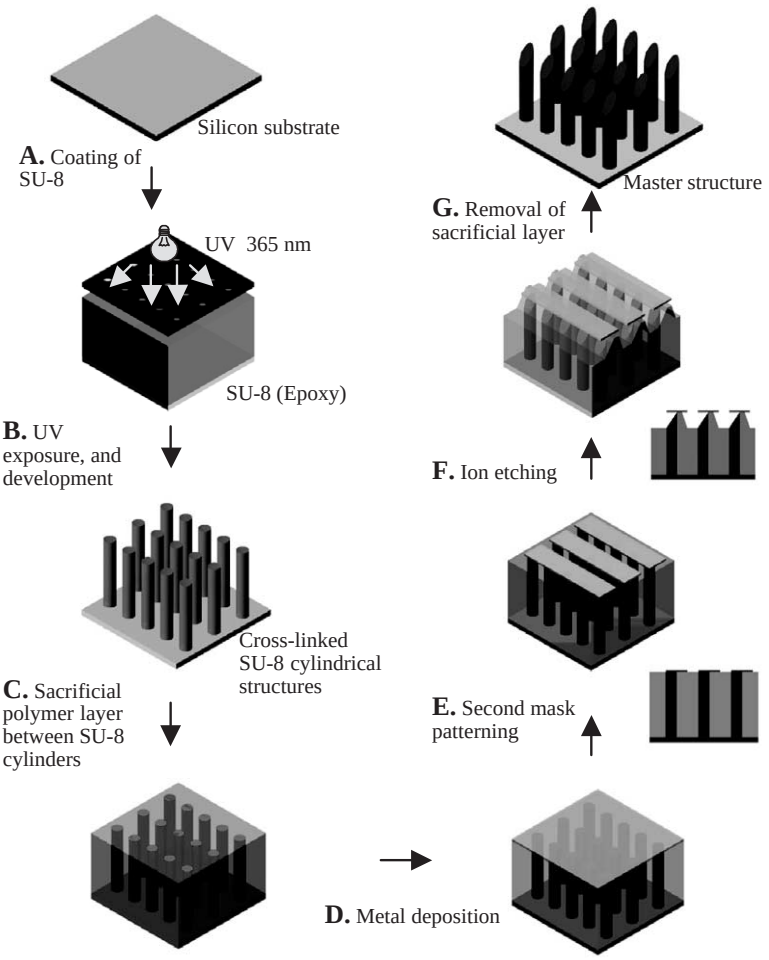

Fig. 1. Schematic of process to fabricate beveled-tip microneedles. SU-8 photoresist is lithographically defined and developed to yield an array of cylinders. After filling the spaces between cylinders with a sacrificial polymer and lithographically placing a metal mask asymmetrically on top of each row of cylinders, the cylinders are ion etched to produce an array of microneedles with beveled tips to be used as a master structure for subsequent molding.

was removed by reactive ion etching with an oxygen plasma to leave a PDMS-silicon mold. Subsequently, polyurethane (Poly 15, Polytek, Easton, PA) was poured into the mold and crosslinked to form polymeric microneedles with chisel tips. Removal of these needles from the mold yielded the final master structure.

2.1.3. Tapered-cone master structures

Tapered-cone microneedles were fabricated using a novel lens-based technique (Fig. 3). A 5300 Å thick, opaque chromium layer was sputter-deposited and lithographically patterned on a glass substrate (soda-lime glass; Telic, Palm Beach Garden, FL) for form a 20×10 array of circular dots each measuring 100 μm in diameter with 400 μm center-to-center spacing. Glass etchant ($HF:HCl:H_2O$ at a volumetric ratio of 1:2:17) was used to isotropically etch the glass substrate through the openings in the patterned chromium layer to create concave holes in the glass of 70 μm radius/depth. Casting of SU-8 photoresist with photoinitiator created a 1000- or 1500-μm thick film on the substrate with bumps that filled the concave holes.

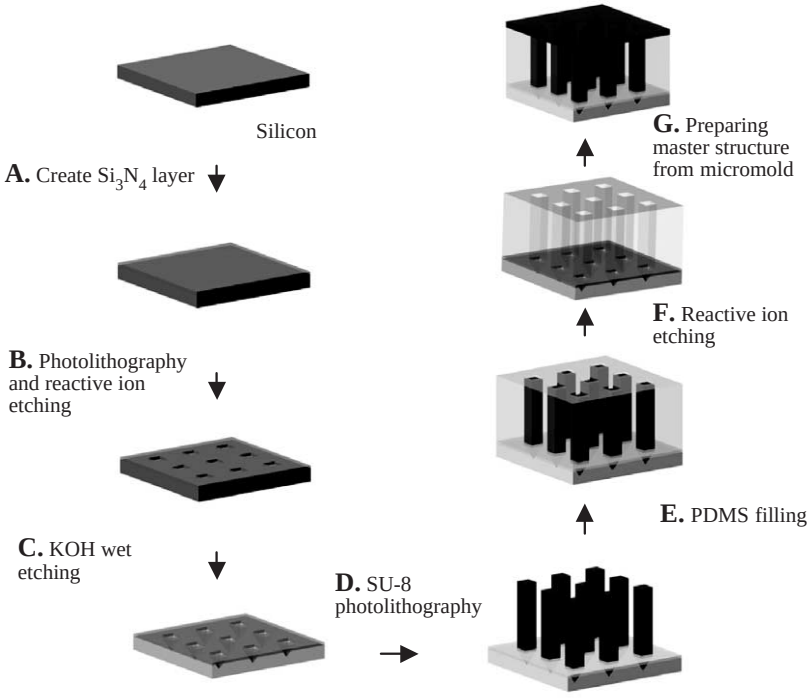

Fig. 2. Schematic of process to fabricate chisel-tip microneedles. Using a lithographically defined Si_3N_4 mask, inverted pyramids are wet-etched into a <1,0,0> silicon substrate. SU-8 photoresist is lithographically patterned into each pyramid hole and as square columns on top. After surrounding the array of SU-8 structures with PDMS and removing SU-8 by reactive ion etching, the resulting mold is used to form an array of chisel-tip microneedles out of polyurethane to be used as a master structure for subsequent molding.

After soft-baking (100 °C, 12 h), the film was exposed from the bottom (through the glass substrate) to UV light. Due to the refractive index difference between the glass substrate and SU-8 resist, the bumps formed integrated microlenses. Light was blocked from passing through the areas between the microlenses due to the opaque chromium layer. Light shining through the lenses was focused within the SU-8 film to give latent images in the shape of tapered cones with a base diameter equal to the circular dot diameter of the chromium mask (i.e., 100 μm) and a length of, for example, 1000 μm, as determined by microlens geometry. Subsequent development of the unexposed SU-8 left a master structure of tapered-cone microneedles.

2.1.4. Micromolding methods

To make molds for replication, these master-structure arrays of SU-8 or polyurethane needles were coated with PDMS (10 mm thick; Sylgard 184, Dow Corning) and allowed to cure for 12 h at 40 °C. After removing the master structures, the molds were covered with pellets of biocompatible polymer—polylactic acid (L-PLA, 1.1 dL/g), polyglycolic acid (PGA, 1.4–1.8 dL/g), or polylactic-co-glycolic acid (PLGA 50/50, 0.5 and 1.2 dL/g) (BPI, Birmingham, AL)—and placed in a vacuum oven (1415M, VWR, West Chester, PA) under −70 kPa vacuum for 5 min at 140, 230 or 180 °C, respectively. Vacuum was applied to remove entrapped bubbles and help pull the polymer melt into the mold. The oven temperatures were selected to be just above the polymer melting points. The samples were then put into the freezer at −20 °C for 30 min before releasing the polymer needles from the PDMS mold by hand. The final polymer needles were stored in a desiccated container in the refrigerator for future use. The molds were also saved for re-use.

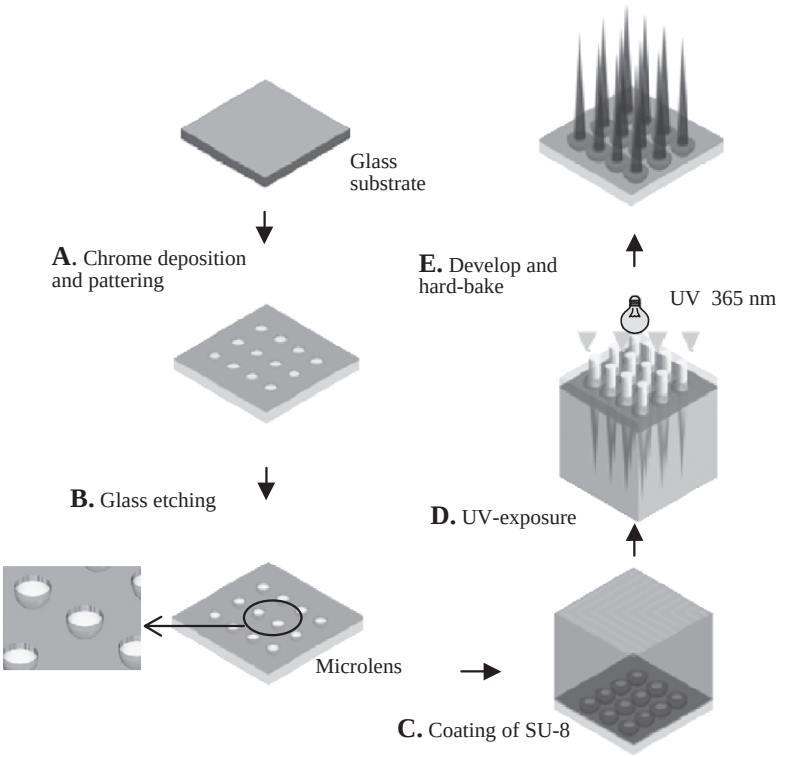

Fig. 3. Schematic of integrated lens process to fabricate tapered-cone microneedles. Using a lithographically defined metal mask, a glass substrate is wet-etched to produce an array of hemispherical invaginations that form microlenses. After filling and covering these invaginations with a thick layer of SU-8 photoresist, UV light is shined through the glass substrate, forming latent images in the SU-8 layer that define the shape of an array of tapered-cone microneedles produced after development that are used as a master structure for subsequent molding.

2.2. Microneedle mechanics and transdermal delivery

2.2.1. Microneedle failure force measurement

Mechanical failure of microneedles was considered due to axial loading and transverse loading. To measure the force a microneedle can withstand before failure under an axial load (i.e., force applied parallel to the microneedle axis), the method of Davis et al. [30] was adapted using a displacement-force test station (Model 921A, Tricor Systems, Elgin, IL). Stress versus strain curves were generated by measuring force and displacement while the test station pressed an array of microneedles against a rigid metal surface at a rate of 1.1 mm/s, as shown in Fig. 4(A). Upon needle failure, the force suddenly dropped; the maximum force applied immediately before dropping was interpreted as the force of needle failure.

As shown in Fig. 4(B), needles were examined by microscopy (IX-70, Olympus, Melville, NY) before and after failure testing to determine the mode of failure, e.g., buckling failure due to inelastic or elastic instability. In most cases, failure was observed for all needles in an array. Data were discarded if only some of the needles were broken. Data are reported as the force per needle required for failure. Using arrays ranging from 20 to 60 needles at a needle density of 300 needles/cm^2, this per-needle normalization accounted for the data, as shown in results section.

To measure the failure force under a transverse load, a row of 5–10 microneedles was mounted vertically on a metal plate using epoxy adhesive (Pacer Technology, Rancho Cucamonga, CA). To apply the transverse load, a glass slide was prepared by bonding a PDMS film ($1 \times 1 \times 0.5$ cm) with cyanoacrylate adhesive (Instant Krazy glue, Elmer's

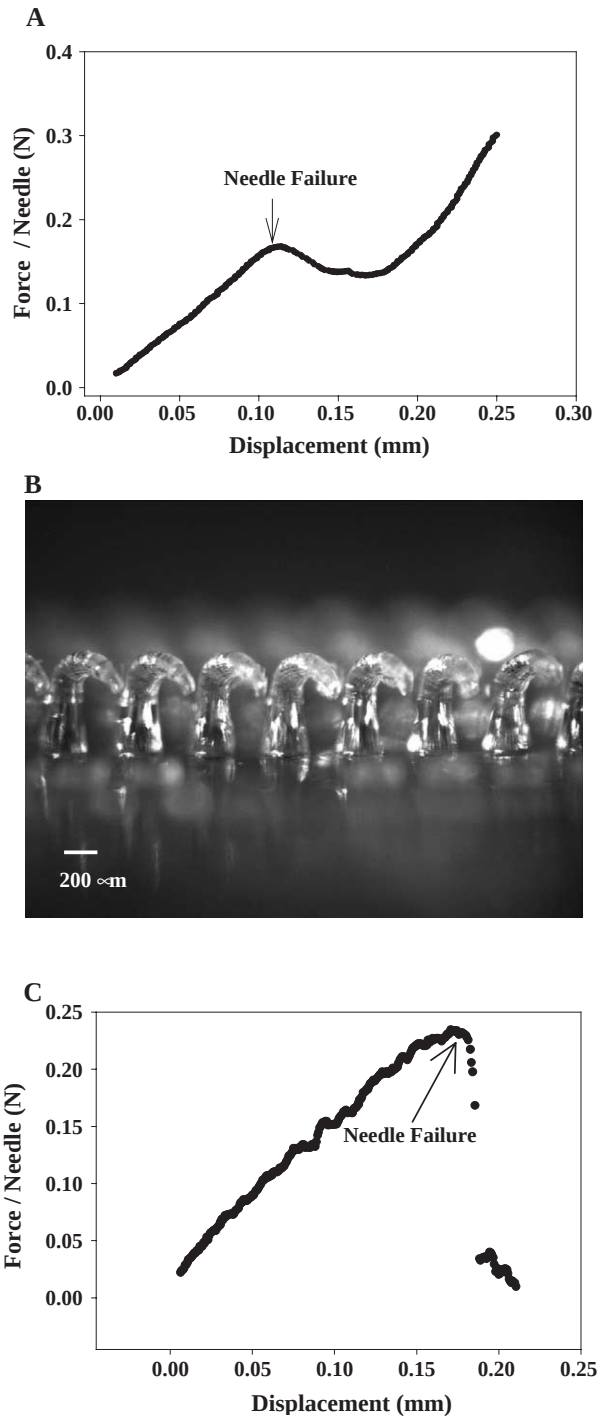

Fig. 4. Mechanical analysis of microneedles. (A) Typical failure behavior of microneedles under axial load. Needle failure is identified by a sudden drop in force. (B) Light micrograph of microneedles after an axial failure test. All microneedles were pressed and deformed with the same magnitude across the whole array. (C) Typical failure behavior of microneedles under transverse load. Needle failure is identified by a sudden drop in force.

Products, Columbus, OH) to the glass slide to make a stepped structure. The PDMS film extended 500 μm beyond the edge of the glass slide to provide a surface of defined dimensions. Using the force displacement–force test station, the PDMS extension from the glass slide was pressed perpendicular to the microneedle axis against a 500 μm length of the microneedle shaft starting at the needle tip. As shown in Fig. 4(C), needle force and displacement were continuously measured until the needles were broken, as verified by microscopy.

2.2.2. Skin permeability measurement

To measure changes in skin permeability after treatment with microneedles, we used standard protocols from the transdermal drug delivery literature [4] adapted to microneedles studies [8,12]. Briefly, heat-stripped epidermis from human cadavers (Emory University Body Donor Program, Atlanta, GA) [38] was used because the stratum corneum (i.e., the upper layer of the epidermis) provides the primary barrier to transdermal transport [4], as well as the main mechanical barrier to needle insertion [39].

After the epidermis was placed on ten layers of tissue paper (Kimwipes, Kimbery-Clark, WI) to provide a tissue-like mechanical support, a 5×20 array of beveled-tip, PGA microneedles was pierced into the epidermis using a force of 4 N, left in place for 3 s, and removed. The epidermis was then placed onto a support mesh (300 μm polypropylene woven screen cloth; Small Parts, Miami Lakes, FL) and loaded into a Franz diffusion chamber (Permegear, Hellertown, PA), which was immersed in a 37 °C water bath (Cole Parmer, Vernon Hills, IL) containing magnetic stirrers (Immersible multi-stirrer, Cole Parmer). The lower, receptor compartment was filled with 5 ml of well-stirred phosphate buffer saline (PBS; Sigma Chemical, St. Louis, MO) in contact with the underside of the viable epidermis. The exposed skin area was 1.8 cm^2.

The upper, donor compartment in contact with the stratum corneum was initially filled with PBS for 5 h to permit skin hydration, after which it was filled with 2 ml of either 1 mM calcein (Sigma Chemical) or 1 mM fluorescein-conjugated bovine serum albumin (BSA conjugated with Texas Red; Molecular Probes, Eugene, OR) in PBS. One hour later, 1 ml of receptor solution was sampled and fluorescence intensity was measured using calibrated spectrofluorometry (QM-1; Photon Technology International, South Brunswick, NJ). Skin permeability was calculated assuming steady state transport across skin [8,12].

2.2.3. Imaging microneedle–skin insertion

To image microneedle insertion into skin, we inserted an array of microneedles into heat-stripped human epidermis as discussed above and either removed the needles to image the residual holes or left the needles in place to image the needles in situ. After needles were removed, a hydrophobic dye (0.4% Trypan blue solution, Sigma Chemical) was applied to the epidermis for 10 min and then patted dry with a tissue wipe. The underside of epidermis was imaged by light microscopy (Olympus SZX12) to determine if dye crossed the skin at the sites of microneedle insertion. The microneedles were also viewed by light microscopy to determine if needles were damaged.

When microneedles were inserted and left in situ, the epidermis with needles was embedded in 30% formaldehyde (Sigma Chemical) for 6 h and then rinsed with DI water. Skin samples were dried using an ethanol substitution process [40], after which ethanol remaining in skin was removed by vacuum drying (Laboport, KNF Neuberger, Trenton, NJ). After gold coating using a sputter coater (Ernest F. Fullam, Latham, NY), skin-needle samples were imaged by scanning electron microscopy (Hitachi 3500 H, Tokyo, Japan).

3. Results and discussion

3.1. Fabrication of sharp-tipped polymer microneedles

To construct microneedles made of polymer strong enough to insert into skin without breaking, three different fabrication methods were developed in this study to produce microneedles with sharp tips to reduce the force to pierce into skin: beveled-tip, chisel-tip and tapered-cone microneedles. The master structures were fabricated out of SU-8 epoxy using lithography and reactive ion etching. After making PDMS molds from these masters, replicate

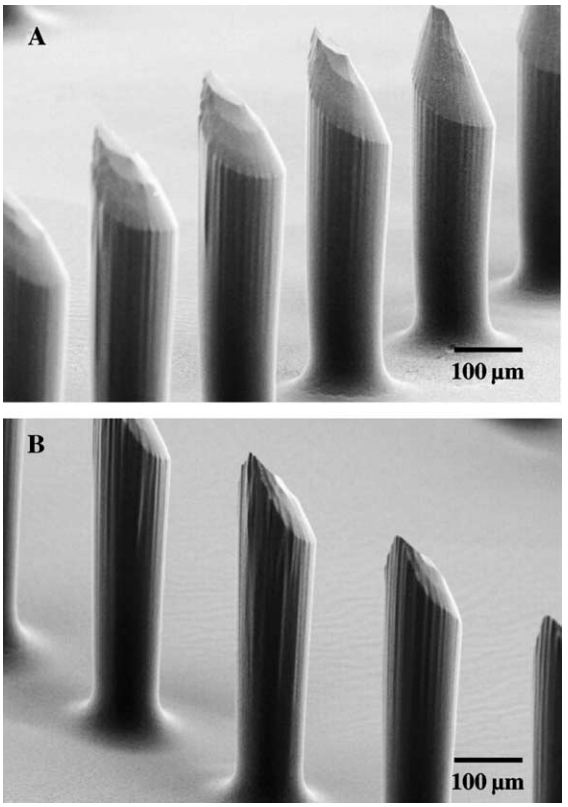

Fig. 5. Beveled-tip microneedles. Scanning electron microscope (SEM) images of a portion of a 120-needle array of PGA microneedles viewed from two different angles. The needle shaft is of approximately constant diameter (100 μm) and then tapers to an asymmetrically beveled tip with a diameter of 10 μm. Needle length is 600 μm.

structures were produced by a modified injection molding technique.

Using the method described in Fig. 1, arrays of beveled-tip microneedles made of polyglycolic acid were fabricated, as shown in Fig. 5. These microneedles were created by molding and replicating master structures fabricated by etching the tips of cylindrical posts made of SU-8 photoresist. The resulting needles are 600 μm in height, 100 μm at their bases, and 10 μm at their tips as part of a 120-needle array. The entire array occupies an area of 9×9 mm. The geometry of a microneedle array—including needle-to-needle spacing, shaft diameter and shape, and tip diameter and shape—can be controlled by adjusting the size, shape and spacing of the lithographic mask. The needle height can be controlled by changing the thickness of SU-8 casting and RIE etching parameters. The tip sharpness can be controlled by optimizing etching parameters.

Using the method described in Fig. 2, arrays of chisel-tip microneedles have also been fabricated, as shown in Fig. 6. Fabrication of the master structures for these needles involved a two-step process. First, the chisel-tips were fabricated as inverted pyramids wet-etched into silicon and then needle shafts were lithographically formed using polymer etching. Fig. 6(A) shows an array of PDMS micropyramids made from the inverted pyramid tip molds. Fig. 6(B) shows an array of chisel-tip microneedles made of polyurethane. Each needle measures 570 μm in height and 100 μm in base width, and is arranged in a 15×15 array with 600-μm center-to-center spacing. The tip

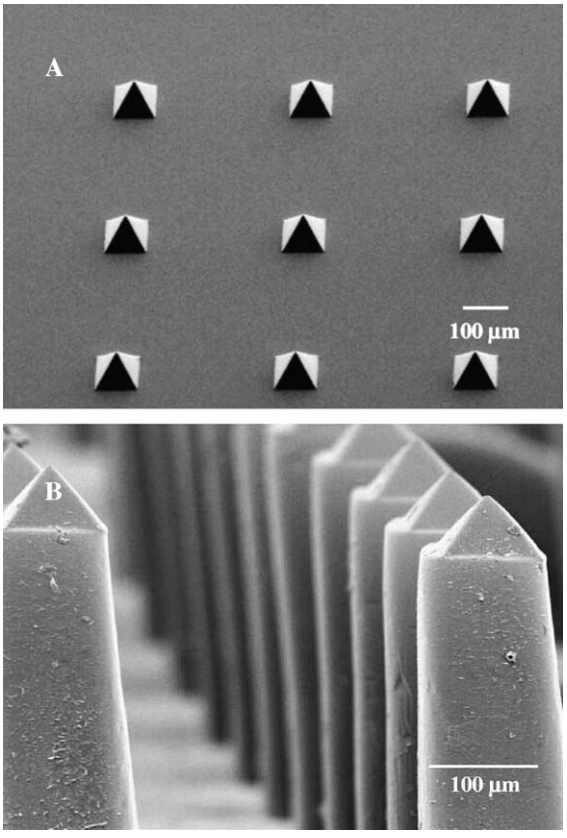

Fig. 6. Chisel-tip microneedles. SEM images of a portion of a 225-needle array of (A) PDMS micropyramid structures formed from a silicon mold to show the geometry of chisel tips and (B) full PGA chisel-tip microneedles with a square shaft of 100 μm width, 570 μm height and a chisel tip terminating at a 10 μm wide tip.

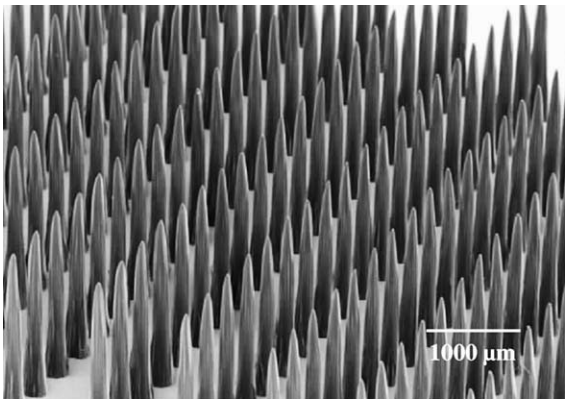

Fig. 7. Tapered-cone microneedles. SEM image of a portion of a 200-needle array of PGA microneedles with a base diameter of 200 μm that taper to a tip diameter of 20 μm over a needle length of 1.5 mm.

angle of 55° is determined by etching along the crystal planes of <1,0,0> silicon. All other geometric properties of the array can be controlled by changing the layout of the lithographic mask.

Using the method described in Fig. 3, tapered-cone microneedles were fabricated with especially large aspect ratios. By first using wet etching to form lenses in a glass substrate, continuously tapered needle master structures were formed by focusing a lithographic pattern into SU-8 photoresist. To demonstrate that this approach especially lends itself to high-aspect-ratio structures, Fig. 7 shows part of a 200-needle array containing 1.5-mm long microneedles fabricated with a base diameter of 200 μm and tip diameter of 20 μm; this yields a length-to-tip diameter aspect ratio of 75. Changing lens geometry and refractive index can be used to control geometric properties of the needles.

3.2. Molding of microneedles

All microneedles developed in this study were made by replicating master structures using PDMS molds. PDMS is commonly used to prepare micromold microdevices, because it (i) has a low surface energy (21.6 dyne/cm), (ii) is usually chemically inert, (iii) is non-hygroscopic, (iv) has good thermal stability, (v) is optically transparent down to wavelengths of ~300 nm, (vi) is mechanically durable and, (vii) is an elastomer with 0.5 MPa Young's modulus [41,42]. However, because it is easily deformable, PDMS is not suitable for conventional injection molding. We therefore developed a modified injection molding technique that applies a vacuum instead of high pressure to fill the mold. It is carried out in a vacuum oven at a temperature just above the polymer melting point. As air is removed from the invaginations of the mold under vacuum, the polymer melt flows into the empty cavities and fills the mold.

Fig. 8 demonstrates the need to apply vacuum in order to fill the mold. Fig. 8(A) shows "microneedles" that result from melting PLGA onto a tapered-cone microneedle mold without applying vacuum. The polymer melt entered the base of microneedle mold cavities, but did not fill the mold. When the same procedure was followed with the addition of applying

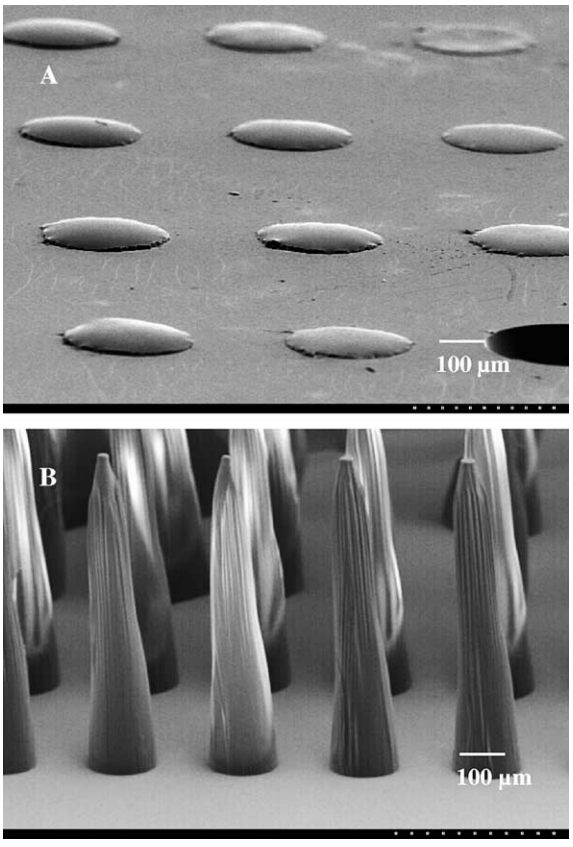

Fig. 8. Modified injection molding technique. SEM images of a portion of 200-needle arrays of (A) partially copied microneedles molded without applying vacuum and (B) fully copied microneedles molded under vacuum.

a vacuum of −70 kPa, Fig. 8(B) shows that the complete needle structures were copied and then released from the mold without breaking.

3.3. Microneedle mechanics

To determine if polymer microneedles are strong enough to insert into skin without breaking, the force required to cause needle failure by axial loading was measured as a function of needle length, base diameter, and Young's modulus using tapered-cone microneedles. Fig. 9(A) shows the failure force for PLGA needles of different length (700, 1000 and 1500 μm) at constant tip diameter (25 μm) and base diameter (200 μm). Failure force decreased with increasing needle length over a range of 0.10–0.22 N/needle (ANOVA, $p < 0.001$). This dependence is expected, because the critical load at which a column fails by buckling is theoretically known to decrease with increasing column length [43].

The significance of these failure force measurements is best appreciated when compared to the force required to insert microneedles into skin. In a separate study [30], insertion force was shown to depend on the interfacial needle area at the tip, where other needle geometric parameters are less important. Because all three needle geometries tested in Fig. 9(A) have a tip diameter of 25 μm and therefore an interfacial area of 490 μm^2, they should all require the same insertion force, which is expected to be 0.058 N/needle [30]. Based on this calculation, the safety factor—defined as the ratio of failure force to insertion force—is always well above unity in Fig. 9(A), decreasing from 3.8 to 1.7 with increasing microneedle length. This suggests that polymer microneedles have sufficient mechanical strength to insert into skin without breaking. This expectation is experimentally validated further below.

Continuing the failure force study, the effect of microneedle diameter was assessed by preparing needles with different base diameters (100 and 200 μm) at constant tip diameter of 25 μm and length of 700 μm. As shown in Fig. 9(B), the failure force increased with base diameter. This dependence is expected, because the critical buckling load is theoretically known to increase as a strong function of column diameter [43]. Again, safety margins greater than unity are predicted in both cases.

Finally, the effect of Young's modulus (and yield strength) on the failure force of needles with 25 μm tip diameter, 200 μm base diameter and 1 mm length was investigated using different polymer materials (Fig. 9(C)). Failure force increased from 0.06 to 0.32 N/needle when increasing Young's modulus from approximately 1 GPa (30 MPa yield strength) for low-molecular weight PLGA to 10 GPa (90 MPa yield strength) for PGA. Consistent with theory [43], the polymers with greater mechanical strength had larger failure forces, which produced safety ratios well above unity for three of the four needle materials tested. However, the low-molecular weight PLGA had a safety ratio close to unity, indicating a poor design for microneedles intended to insert into skin.

The force required to cause microneedle failure by a transverse load was also measured. Using PGA needles of constant tip diameter (25 μm) and length (1 mm) the average failure force was found to be 0.058 ± 0.012 and 0.24 ± 0.05 N for needles of 100 and 200 μm base diameters, respectively. Considering the 200 μm base diameter needle, the transverse-load failure force is smaller than the axial-load failure force for microneedles of same geometry and material. This indicates that if microneedles experience a significant transverse load due to incorrect axial insertion into skin or skin deformation during insertion, microneedles could fail by transverse bending.

3.4. Increased skin permeability

To test the ability of polymer microneedles to increase transdermal drug delivery, the ability of polymer microneedles to pierce into skin was assessed first. An array of beveled-tip microneedles was inserted into the epidermis of human cadaver skin and then removed. After briefly applying Trypan blue dye to the outer, stratum corneum side of the skin and then wiping it off, the inner, viable epidermis side of the skin was examined by light microscopy to image sites where microneedles increased skin permeability and thereby permitted transport of the dye into the skin. Fig. 10(A) contains a representative optical photomicrograph that shows the resulting array of blue dots on the underside of epidermis in the same shape and location as the needle array. This indicates that the polymer microneedles successfully inserted into skin without breaking, as confirmed by subse-

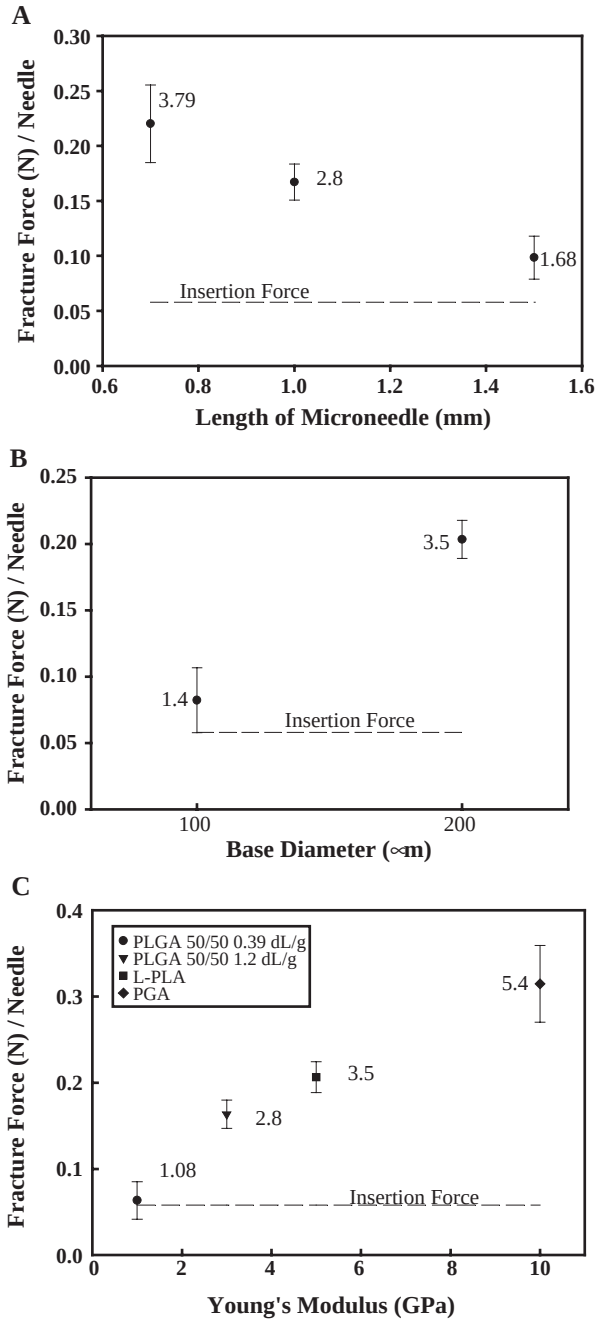

Fig. 9. Mechanical strength of polymer microneedles. The force required to fracture a needle in an array of 30–35 microneedles is shown as a function of (A) needle length (200 μm base diameter, 25 μm tip diameter, PLGA 50/50 (1.2 dL/g) held constant), (B) base diameter (25 μm tip diameter, 700 μm length, PLGA 50/50 (1.2 dL/g)) and (C) Young's modulus (25 μm tip diameter, 200 μm base diameter, 1 mm length) achieved using low-molecular weight PLGA (Young's modulus, $E=1$ GPa; yield strength, $\sigma=30$ MPa), high-molecular weight PLGA ($E=3$ GPa; $\sigma=50$ MPa), PLA ($E=5$ GPa; $\sigma=70$ MPa) and PGA ($E=10$ GPa; $\sigma=90$ MPa) [32,47]. Expected insertion forces are indicated by the dashed lines, as determined from a previous study [30]. The ratio of the fracture force to insertion force—termed the safety factor—is shown next to each data point. Data points represent the average of nine measurements with error bars corresponding to the standard deviation.

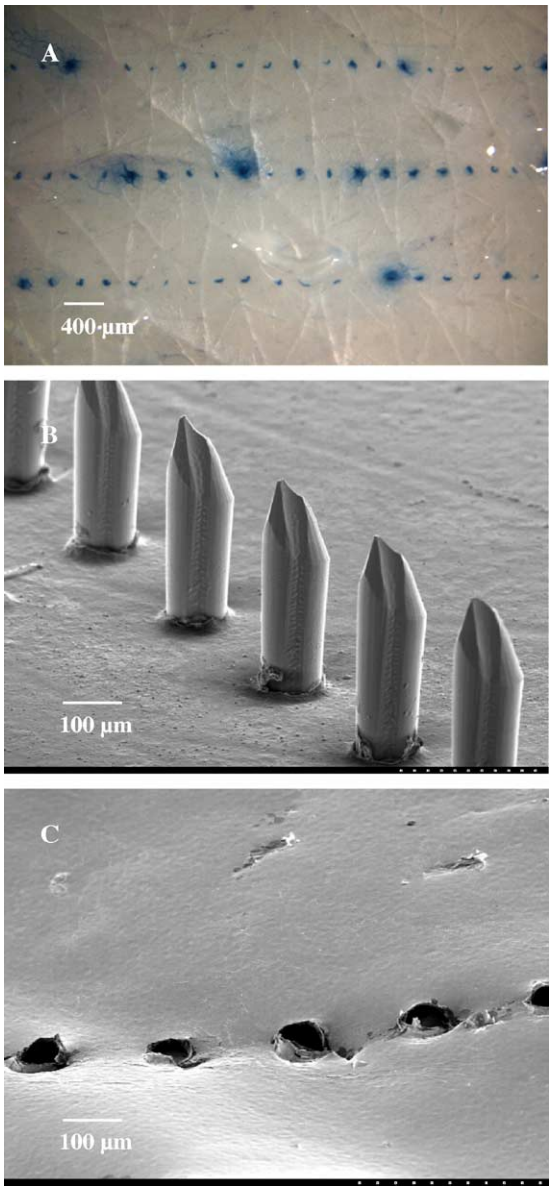

Fig. 10. Holes pierced across human cadaver skin. (A) Optical micrograph of the underside of human cadaver epidermis pierced by an array of polymer microneedles and subsequently exposed to Trypan blue dye. The pattern of dye staining is the same as the array of microneedles, indicating that microneedles pierced the skin and created pathways for dye transport across the skin. (B) Microneedles pierced across human cadaver epidermis and imaged in situ by SEM. Microneedles remained intact after insertion. To prepare for imaging, the skin was dehydrated, which caused it to collapse down to the base of the microneedles. These microneedles contain a notch intentionally placed along the needle shaft (see text). (C) SEM image of human cadaver epidermis after microneedles were inserted and removed. The residual holes in skin are evident.

quent microscopic examination of the needles afterwards, and increased skin permeability in a highly localized manner at the sites of needle insertion.

To provide additional visual evidence that polymer microneedles insert into skin, beveled-tip polymer microneedles were inserted into epidermis and left in place. The needles used in this case were notched along the sides, which may be of use in future applications as a conduit for drug transport while needles remain inserted within skin. After chemically fixing and dehydrating the skin, Fig. 10(B) shows fully intact needles that pierced through the epidermis. In this image, the epidermis is dehydrated and therefore has collapsed down to the base of the microneedles. Fig. 10(C) shows a companion image of skin taken after needles were inserted and removed from skin before fixation and dehydration, showing residual holes in the skin.

To quantify changes in transdermal transport caused by polymer microneedles, the permeability of intact human cadaver epidermis to calcein (623 Da; 0.6 nm radius) and bovine serum albumin (66 kDa; 3.5 nm radius) was compared to the permeability of epidermis pierced with arrays of 20 or 100 microneedles. As seen in Fig. 11, insertion and removal of an array of 20 polymer microneedles increased skin

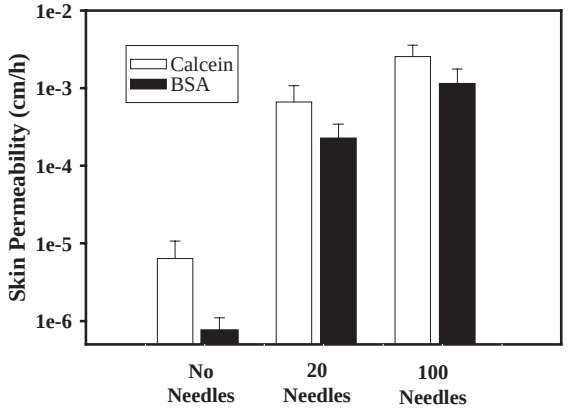

Fig. 11. Increased skin permeability after piercing with microneedles. Permeability of human cadaver epidermis is shown for calcein (white bars) and bovine serum albumin (black bars) for intact skin (i.e., “no needles”) and for skin pierced with an array of either 20 or 100 beveled-tip PGA microneedles. The microneedles were 600 μm tall, 100 μm in diameter at their base, and 10 μm wide at their tips. The needles were positioned in a 20 × 6 array with a center-to-center spacing of 400 and 1400 μm.

permeability to calcein and BSA by at least two orders of magnitude (Student's t-test, $p<0.006$), while a 100-needle array increased permeability by almost three orders of magnitude (Student's t-test, $p<0.004$). There is also a statistically significant effect of the number of needles used, where an array of 100 microneedles increased permeability four-fold more than 20 microneedles for both calcein and BSA (Student's t-test, $p<0.006$). These substantial increases in skin permeability are significant for transdermal drug delivery applications and are similar to increases previously observed in experiments with solid silicon microneedles [12].

3.5. Discussion of significance

The work performed in this study has significance to both microfabrication and drug delivery. First, the desire to have polymer microneedles and the need for them to have sharp tips motivated the development of three new methods to fabricate microneedles. Asymmetric masking during reactive ion etching led to beveled-tip microneedles and wet-etching along <1,0,0> silicon crystal planes led to chisel-tip microneedles. While these fabrication tools have been used before in other contexts [22,24], this study presents their first application to polymer microneedles. Additionally, tapered-cone microneedles were fabricated using a novel lens-based technique, which is a new method to the field of microfabrication [36].

The molding approach described here is also of potential significance. The use of PDMS molds to replicate microstructures has already found widespread application [44], but filling these molds, especially when they have high aspect ratio feature sizes, is a persistent problem. In this study a novel vacuum-based method is presented to fill molds with aspect ratios as large as 75, as in the case of our longest tapered-cone needles. This modified injection molding technique could find additional applications in a variety of micromolding scenarios.

Specifically concerning microneedles, most previous work has studied fabrication using silicon or metal. However, silicon is more expensive than commodity metals and polymers, is relatively brittle, and is not an established biomaterial with an FDA track record [28]. Metals are more appropriate materials for microneedles, given the low cost, strength, and precedent in FDA-approved devices [29]. However, even a low incidence of metal needle fracture in the high-volume applications envisioned for microneedles is a safety concern.

The use of polymer microneedles described in this study may provide advantages that overcome limitations of silicon and metal. Many polymer materials are inexpensive, mechanically strong, and enjoy a long-standing safety record in medical devices [29]. Moreover, the biodegradable polymers used here further alleviate issues of safety, because broken needles left embedded in the skin can safely degrade and disappear. Safe disposal of polymer microneedles is also facilitated by the ability to burn, dissolve in a solvent, or mechanically destroy needles to prevent intentional or accidental re-use; destruction of used needles in developing countries is a high priority of the U.S. Centers for Disease Control and Prevention, the World Health Organization, and other international agencies [45].

Finally, the ability of polymer microneedles to increase skin permeability by orders of magnitude has significant potential impact in medicine. Previous studies using microneedles made of other materials have demonstrated delivery of proteins, DNA, vaccines and other compounds both in vitro and in vivo [9,10]. Similar performance observed here for delivery of calcein and bovine serum albumin suggests that polymer microneedles might be used to deliver a wide variety of drugs, with the added safety and fabrication advantages of biodegradable polymer materials. Moreover, previous studies have shown that silicon microneedles can be painless [46]. Preliminary studies indicate that the polymer microneedles used in this study can similarly be inserted into skin without pain (data not shown).

4. Conclusion

This study demonstrates that microneedles can be made out of biodegradable polymers. Sharp tips were achieved by adapting microfabrication techniques to produce beveled- and chisel-tip microneedles and developing a novel fabrication method to produce tapered-cone microneedles. Microfabricated master structures were replicated using PDMS molds and a novel vacuum-based method to fill the molds with

biodegradable polymer melts. This fabrication method is expected to be suitable for rapid scale-up for inexpensive, mass production. Mechanical testing showed that the force required to cause microneedle failure increased by making microneedles of shorter length, wider base diameter, and larger Young's modulus and yield strength. Failure forces ranged from 0.06 to 0.32 N/needle. Almost all of the microneedle designs tested had failure forces much greater than their expected insertion forces, yielding safety ratios as large as 5.4. When inserted into human cadaver skin, polymer microneedles were shown to create pathways for transdermal transport that increased skin permeability to calcein and bovine serum albumin by up to three orders of magnitude. Altogether, these results show that biodegradable polymer microneedles can be fabricated using manufacturable microfabrication techniques, have sufficient mechanical strength to insert into skin with a wide safety margin, and dramatically increase skin permeability to levels of interest for drug delivery applications.

Acknowledgements

We thank Devin McAllister, Yong-Kyu Yoon, Shawn Davis, Wijaya Martanto, and Harvinder Gill for helpful discussions. This work was supported in part by the National Institutes of Health, National Science Foundation, American Diabetes Association, and DARPA.

References

[1] R. Langer, Drug delivery and targeting, Nature 392 (1998) 5–10.
[2] K. Park, Controlled Drug Delivery: Challenges and Strategies, American Chemical Society, Washington, DC, 1997.
[3] M.R. Prausnitz, S. Mitragotri, R. Langer, Current status and future potential of transdermal drug delivery, Nat. Rev. Drug. Discov. 3 (2004) 115–124.
[4] R.L. Bronaugh, H.I. Maibach, Percutaneous Absorption: Drugs–Cosmetics-Mechanisms–Methodology, Marcel Dekker, New York, 1999.
[5] C.H. Purdon, C.G. Azzi, J. Zhang, E.W. Smith, H.I. Maibach, Penetration enhancement of transdermal delivery—current permutations and limitations, Crit. Rev. Ther. Drug Carrier Syst. 21 (2004) 97–132.
[6] H. Schaefer, T.E. Redelmeier, Skin Barrier: Principles of Percutaneous Absorption, Karger, Basel, Swizerland, 1996.
[7] A. Joshi, J. Raje, Sonicated transdermal drug transport, J. Control. Release 88 (1) (2002) 13–22.
[8] S. Henry, D.V. McAllister, M.G. Allen, M.R. Prausnitz, Microfabricated microneedles: a novel approach to transdermal drug delivery, J. Pharm. Sci. 87 (8) (1998) 922–925.
[9] M.R. Prausnitz, Microneedles for transdermal drug delivery, Adv. Drug Deliv. Rev. 56 (2004) 581–587.
[10] M.R. Prausnitz, J.A. Mikszta, J. Raeder-Devens, Microneedles, in: E.W. Smith, H.I. Maibach (Eds.), Percutaneous Penetration Enhancers, CRC Press, Boca Raton, FL, in press.
[11] M.L. Reed, W.K. Lye, Microsystems for drug and gene delivery, Proc. IEEE 92 (1) (2004) 56–75.
[12] D.V. McAllister, P.M. Wang, S.P. Davis, J.H. Park, P.J. Canatella, M.G. Allen, M.R. Prausnitz, Microfabricated needles for transdermal delivery of macromolecules and nanoparticles: fabrication methods and transport studies, Proc. Natl. Acad. Sci. U. S. A. 100 (2003) 13755–13760.
[13] W. Lin, M. Cormier, A. Samiee, A. Griffin, B. Johnson, C.L. Teng, G.E. Hardee, P.E. Daddona, Transdermal delivery of antisense oligonucleotides with microprojection patch (Macroflux) technology, Pharm. Res. 18 (12) (2001) 1789–1793.
[14] M. Cormier, P.E. Daddona, Macroflux technology for transdermal delivery of therapeutic proteins and vaccines, in: M.J. Rathbone, J. Hadgraft, M.S. Roberts (Eds.), Modified-Release Drug Delivery Technology, Marcel Dekker, New York, 2003, pp. 589–598.
[15] M. Cormier, B. Johnson, M. Ameri, K. Nyam, L. Libiran, D.D. Zhang, P. Daddona, Transdermal delivery of desmopressin using a coated microneedle array patch system, J. Control. Release 97 (3) (2004) 503–511.
[16] W. Martanto, S.P. Davis, N. Holiday, J. Wang, H. Gill, M.R. Prausnitz, Transdermal delivery of insulin using microneedles in vivo, Pharm. Res. 21 (2004) 947–952.
[17] F. Chabri, K. Bouris, T. Jones, D. Barrow, A. Hann, C. Allender, K. Brain, J. Birchall, Microfabricated silicon microneedles for nonviral cutaneous gene delivery, Br. J. Dermatol. 150 (2004) 869–877.
[18] J.A. Mikszta, J.B. Alarcon, J.M. Brittingham, D.E. Sutter, Improved genetic immunization via micromechanical disruption of skin-barrier function and targeted epidermal delivery, Nat. Med. 8 (4) (2002) 415–419.
[19] J.A. Matriano, M. Cormier, J. Johnson, W.A. Young, M. Buttery, K. Nyam, P.E. Daddona, Macroflux microprojection array patch technology: a new and efficient approach for intracutaneous immunization, Pharm. Res. 19 (1) (2002) 63–70.
[20] S.P. Davis, W. Martanto, M.G. Allen, M.R. Prausnitz, Transdermal insulin delivery to diabetic rats through microneedles, IEEE Trans. Biomed. Eng. (in press).
[21] J.G.E. Gardeniers, R. Luttge, A. Van der Berg, J.W. Berenschot, M.J. de Boer, Y. Yeshurun, M. Hefetz, R. van't Oever, Silicon micromachined hollow microneedles for transdermal liquid transport, J. Microelectromech. Syst. 6 (2003) 855–862.

[22] J.D. Zahn, N.H. Talbot, A.P. Pisano, D. Liepmann, Microfabricated polysilicon microneedles for minimally invasive biomedical devices, Biomed. Microdevices 2 (4) (2000) 295–303.
[23] B. Stoeber, D. Liepmann, Two-dimensional arrays of out of plane needles, Presented at ASME International Mechanical Engineering Congress and Exposition, MEMS, Orlando, FL, 2000.
[24] J.G.E. Gardeniers, A. Van der Berg, J.W. Berenschot, M.J. de Boer, Y. Yeshurun, M. Hefetz, R. van't Oever, Silcon micromachined hollow microneedles for transdermal liquid transfer, Presented at IEEE MEMS 2002 Conference, Las Vegas, NV, 2002.
[25] K. Kim, D.S. Park, H.M. Lu, W. Che, K. Kim, J.B. Lee, C.H. Ahn, A tapered hollow metallic microneedle array using backside exposure of SU-8, J. Micromechanics Microengineering 14 (2004) 597–603.
[26] S. Chandrasekaran, J.D. Brazzle, A.B. Frazier, Surface micromachined metallic microneedles, J. Microelectromech. Syst. 12 (3) (2003) 281–288.
[27] P. Griss, P. Enoksson, G. Stemme, Micromachined barbed spikes for mechanical chip attachment, Sens. Actuators, A, Phys. 95 (2002) 94–99.
[28] W.R. Runyan, K.E. Bean, Semiconductor Integrated Circuit Processing Technology, Addison-Wesley, New York, 1990.
[29] J.H. Braybrook, Biocompatibility: Assessment of Medical Devices and Materials, Wiley, New York, 1997.
[30] S.P. Davis, B.J. Landis, Z.H. Adams, M.G. Allen, M.R. Prausnitz, Insertion of microneedles into skin: measurement and prediction of insertion force and needle fracture force, J. Biomech. 37 (2004) 1155–1163.
[31] P.A. Stupar, A.P. Pisano, Silicon, parylene and silicon/parylene micro-needles for strength and toughness, Presented at Transducers 2001 Conference, Munich, Germany, 2001.
[32] B.D. Ratner, A.S. Hoffman, F.J. Schoen, J.E. Lemons, Biomaterials Science: An Introduction to Materials in Medicine, Academic Press, New York, 1996.
[33] D.V. McAllister, M.G. Allen, M.R. Prausnitz, Microfabricated microneedles for gene and drug delivery, Annu. Rev. Biomed. Eng. 2 (2000) 289–313.
[34] C.G. Ambrose, T.O. Clanto, Bioabsorbable implants: review of clinical experience in orthopedic surgery, Ann. Biomed. Eng. 32 (1) (2004) 171–177.
[35] J.H. Park, M.G. Allen, M.R. Prausnitz, Polymer microneedles for transdermal drug delivery, Presented at the 29th Annual Meeting & Exposition of the Controlled Release Society, Seoul, Korea, 2002.
[36] J.H. Park, Y.K. Yoon, M.G. Allen, M.R. Prausnitz, High-aspect-ratio tapered structures using an integrated lens technique, Presented at IEEE MEMS 2004 Conference, Maastricht, Netherlands, 2004.
[37] K.E. Bean, Anisotropic etching of silicon, IEEE Trans. Electron Devices ED-25 (10) (1978) 1185–1193.
[38] D.W. Hobson, Dermal and Ocular Toxicology: Fundamentals and Methods, CRC Press, Boca Raton, FL, 1991.
[39] B.F. Van Duzee, The influence of water content, chemical treatment and temperature on the rheological properties of stratum corneum, J. Invest. Dermatol. 71 (2) (1978) 40–44.
[40] C.L. Gummer, In vitro evaluation of transdermal delivery, in: J. Hadgraft, R.H. Guy (Eds.), Transdermal Drug Delivery: Development Issues and Research Initiatives, Marcel Dekker, New York, 1989, pp. 177–186.
[41] M.J. Madou, Fundamentals of Microfabrication: The Science of Miniaturization, CRC Press, Boca Raton, FL, 2002.
[42] D. Armani, C. Liu, N. Aluru, Re-configurable fluid circuits by PDMS elastomer micromachining, Presented at IEEE MEMS, Orlando, FL, 1999.
[43] R.L. Mott, Applied Strength of Materials, Prentice Hall, Englewood Cliffs, 1996.
[44] Y. Xia, G.M. Whitesides, Soft lithography, Annu. Rev. Mater. Sci. 28 (1998) 153–184.
[45] L. Simonsen, A. Kane, J. Lloyd, M. Zaffran, M. Kane, Unsafe injections in the developing world and transmission of bloodborne pathogens: a review, Bull. World Health Organ. 77 (1999) 789–800.
[46] S. Kaushik, A.H. Hord, D.D. Denson, D.V. McAllister, S. Smitra, M.G. Allen, M.R. Prausnitz, Lack of pain associated with microfabricated microneedles, Anesth. Analg. 92 (2001) 502–504.
[47] Y. Zhang, D.L. Wise, Y.Y. Hsu, In vitro study of buffered biodegradable fracture fixation device, in: D.L. Wise (Ed.), Biomaterials and Bioengineering Handbook, Marcel Dekker, New York, 1995, pp. 553–576.